Journal of the European Ceramic Society 21 (2001) 545–553

www.elsevier.com/locate/jeurceramsoc

The electrical properties and d.c. degradation characteristics of Dy_2O_3 doped Pr_6O_{11}-based ZnO varistors

Choon-Woo Nahm *

Department of Electrical Engineering, Dongeui University, Pusan 614-714, South Korea

Received 27 April 2000; received in revised form 9 July 2000; accepted 16 July 2000

Abstract

The electrical properties and degradation of Pr_6O_{11}-based varistors, which are composed of ZnO–Pr_6O_{11}–CoO–Dy_2O_3 systems, were investigaed with Dy_2O_3 content. Highly densified ceramics sintered at 1350°C were obtained by doping with 0.5 mol% Dy_2O_3, reaching 97% of theoretical density. The addition of Dy_2O_3 to the ternary system ZnO–Pr_6O_{11}–CoO greatly improved the *V–I* characteristics in terms of with and without Dy_2O_3 addition. The stability of varistors sintered at 1350°C was far higher than that at 1300°C. The varistors with 0.5 mol% Dy_2O_3 showed excellent stability as well as relatively good nonlinear *V–I* characteristics, which are 37.8 in the nonlinear exponent and 5.4 μA in the leakage current. Their variation rate of varistor voltage was −1.7% even under very severe stress (0.80 $V_{1\ mA}$/90°C/12 h) + (0.85 $V_{1\ mA}$/115°C/12 h) + (0.90 $V_{1\ mA}$/120°C/12 h) + (0.95 $V_{1\ mA}$/125°C/12 h).

Keywords: Electrical properties; Dy_2O_3; Leakage current; Varistors; ZnO

1. Introduction

Zinc oxide varistors are ceramic semiconductor devices produced by a ceramic sintering process, based on ZnO with additives of small amounts of varistor-forming oxides, namely, Bi_2O_3 and Pr_6O_{11}. Microstructurally, the sintering process gives rise to a structure, which consist of semiconducting *n*-type ZnO grains surrounded by very thin insulating intergranular layers.[1,2] In other words, ZnO varistors possess a microstructure of three-dimensional series–parallel networks, in which a unit structure of ZnO grain (semiconductor)–intergranular layer (insulator)–ZnO grain (semiconductor) distributes to a specified volume size. A unit structure corresponds to a micro-varistor. Functionally, ZnO varistors exhibit highly nonlinear voltage–current (*V–I*) properties expressed by the relation $I = KV^{\alpha}$, where *K* is a constant and α is a nonlinear exponent, which characterizes the nonlinear properties of varistors. These nonlinear properties essentially result from an electrostatic potential barrier at the active grain boundary, containing many trap states. ZnO varistors are equivalent to a back-to-back Zener diode and are connected in parallel with circuits to protect them from voltage surges. They are always subjected to a voltage below their breakdown voltage and pass a leakage current. When they are subjected to a voltage above their breakdown voltage, they act as conductors, discharging surges to ground. When the voltage returns to the normal state, they again return to a highly resistive state. As a result, ZnO varistors are devices which switch from a highly insulating state to a highly conducting state. Therefore, they are widely used as surge absorbers in electronic circuits and core elements of surge arresters in electric power lines, such as the transmission and distribution lines.

ZnO varistors are largely classified into two categories, called Bi_2O_3-based and Pr_6O_{11}-based varistors, in terms of varistor-forming oxides inducing the nonlinear properties of varistors. Since the discovery of Bi-based ZnO varistors, many researchers have studied the microstructure, electrical conduction, dielectric characteristics, degradation characteristics and mechanisms. Most of the commercial ZnO varistors are Bi_2O_3-based varistors showing excellent properties, but they have a few flaws due to Bi_2O_3 having a high volatility and reactivity.[3] The former changes the varistor characteristics with the

* Corresponding author.
E-mail address: cwnahm@hyomin.dongeui.ac.kr (C.-W. Nahm).

0955-2219/01/$ - see front matter
PII: S0955-2219(00)00233-8

variation of the inter-composition ratio of additives, the latter destroys the multilayer structure of chip varistors, and it generates an additional insulating spinel phase, which does not play any role in electrical conduction. Another flaw of Bi_2O_3-based varistors is that they need many additives to obtain high nonlinearity and stable electrical properties. ZnO varistors generally possess three phases, such as ZnO grains, Bi_2O_3-rich intergranular layer, and spinel particles. It has also been found that they need many additives to obtain a high nonlinear exponent and stable electrical properties. On the other hand, Pr_6O_{11}-based ZnO varistors are reported to have only two-phases, namely, ZnO grains and intergranular layers.[4] The absence of a spinel phase, which does not play an electrical role at the grain boundaries, increases the active grain boundary area through which the electrical current flows. Therefore, the effective cross-section area of the element is increased. This gives rise to compacting of systems, variety in application area, and high performance as a surge protector. To apply Pr_6O_{11}-based varistors in various areas, the effect of the variables, such as the kind and amount of additives, composition ratio, sintering temperature, and cooling rate on the electrical properties, and stability of Pr_6O_{11}-based varistors should be continuously, diversely studied. Most of the studies on Pr_6O_{11}-based varistors, a few years ago, have been limited to the ternary system ZnO–Pr_6O_{11}–CoO and further, no details on their stability has been reported.[5–7] Recently, Y_2O_3-added, Nd_2O_3-added, and Er_2O_3-added ZnO varistors to the ternary system ZnO–Pr_6O_{11}–CoO have been studied for the stability as well as the electrical properties.[8–10] They have exhibited a relatively good electrical performance.

In this paper, the effect of dysprosium oxide (Dy_2O_3) on the electrical properties, such as *I–V* and capacitance–voltage (*C–V*) characteristics, and degradation characteristics of ZnO–Pr_6O_{11}–CoO-Dy_2O_3 based (ZPCD) varistors have been examined with Dy_2O_3 doping and sintering temperatures.

2. Experimental procedure

Reagent-grade raw materials were prepared for ZPCD varistors with composition (98.5−*x*) mol% ZnO, 0.5 mol% Pr_6O_{11}, 1.0 mol% CoO, *x* mol% Dy_2O_3 (*x* = 0.0, 0.5, 1.0, 2.0). Raw materials were mixed by ball milling with zirconia balls and acetone in a polypropylene bottle for 24 h. The mixture was dried at 120°C for 12 h and calcined in air at 750°C for 2 h. The calcined mixture was pulverized using an agate mortar/pestle and after 2 wt.% polyvinyl alcohol (PVA) binder addition, granulated using a sieving 200-mesh screen to produce the starting powder. The powder was pressed into discs of 10 mm in diameter and 2 mm in thickness at a pressure of 80 MPa. The discs were placed in the starting powder using an alumina crucible, sintered at 1300 and 1350°C in air for 1 h, and furnace-cooled to room temperature. The heating and cooling rates were 4°C/min. The as-sintered samples were lapped and polished to 1.0 mm thickness on both surfaces. They were coated with conductive silver paste on both faces, and then ohmic contacts were formed by heating at 600°C for 10 min. The size of electrodes was 5 mm in diameter.

The current–voltage (*V–I*) characteristics of ZPCD varistors were measured using an *I–V* source/measure unit (Keithley 237). The varistor voltage ($V_{1\ mA}$) was measured at 1.0 mA/cm^2 and the leakage current (I_ℓ) was defined as the current at 0.80 $V_{1\ mA}$. In addition, the nonlinear exponent (α) is defined by $\alpha = 1/(\log E_2 - \log E_1)$, where E_1 and E_2 are the electric field corresponding to 1.0 mA/cm^2 and 10 mA/cm^2, respectively. The capacitance–voltage (*C–V*) characteristics of ZPCD varistors were measured at 1 kHz using a RLC meter (QuadTech 7600) and an electrometer (Keithley 617). The donor concentration (N_d) and the barrier height (ϕ_b) were determined by the equation[11] $(1/C_b - 1/(2C_{bo}))^2 = 2(\phi_b + V_{gb})/q\varepsilon N_d$, where C_b is the capacitance per unit area of a grain boundary, C_{bo} is the value of C_b when $V_{gb} = 0$ *V*, V_{gb} is the applied voltage per grain boundary, q is the electronic charge and ε is the permittivity of ZnO ($\varepsilon = 8.5\ \varepsilon_o$).

The density of interface states (N_t) at the grain boundary was determined by the equation[11] $N_t = (2\varepsilon N_d \phi_b/q)^{1/2}$ using the value of the donor concentration and barrier height obtained above. Once the donor concentration and barrier height are known, the depletion layer width (t) of either side at the grain boundaries was determined by[12] the equation $N_d t = N_t$. The degradation tests were performed under the four continuous d.c. stress conditions, such as 0.80 $V_{1\ mA}$/90°C/12 h in the first stress, (0.80 $V_{1\ mA}$/90°C/12 h) + (0.85 $V_{1\ mA}$/115°C/12 h) in the second stress, (0.80 $V_{1\ mA}$/90°C/12 h) + (0.85 $V_{1\ mA}$/115°C/12 h) + (0.90 $V_{1\ mA}$/120°C/12 h) in the third stress, (0.80 $V_{1\ mA}$/90°C/12 h) + (0.85 $V_{1\ mA}$/115°C/12 h) + (0.90 $V_{1\ mA}$/120°C/12 h) + (0.95 $V_{1\ mA}$/125°C/12 h) in the fourth stress, (0.80 $V_{1\ mA}$/90°C/12 h) + (0.85 $V_{1\ mA}$/115°C/12 h) + (0.90 $V_{1\ mA}$/120°C/12 h) + (0.95 $V_{1\ mA}$/125°C/12 h) + (0.95 $V_{1\ mA}$/150°C/12 h) in the fifth stress. And at the same time, the leakage current during the stress time was monitored at intervals of 1 min by an *I–V* source/measure unit (Keithley 237).

The either surface of samples that the electrical measurement has been finished was lapped and ground with SiC paper and polished with 0.3 μm-Al_2O_3 powder to a mirror-like surface. The polished samples were thermally etched at 1100–1150°C for 10–30 min. The surface of samples was metallized with a thin coating of Au to reduce charging effects and to improve the resolution of the image. The surface microstructure was examined by

scanning electron microscopy (SEM, Hitachi S2400, Japan). The average grain size (d) was determined by the lineal intercept method, given by[13] $d = 1.56\ L/MN$, where L is the random line length on the micrograph, M is the magnification of the micrograph, and N is the number of the grain boundaries intercepted by lines. The density of ZPCD ceramics was measured by the Archimedes method.

3. Results and discussion

Fig. 1 shows the density of ZPCD ceramics at 1300 and 1350°C with Dy_2O_3 content. The density of ceramics, in ceramics sintered at 1300°C, was decreased in the range of 4.69 to 4.24 g/cm^3, which is in the range of 81 to 73% of the theoretical density (TD) of pure ZnO and wholly, the density was found to be low. On the other hand, The density of ceramics, in ceramics sintered at 1350°C, was decreased in the range of 5.62 to 4.81 g/cm^3, corresponding to the range of 97 to 83% of TD. The ceramics with 0.5 mol% Dy_2O_3 sintered at 1350°C exhibited the highest densification, reaching 97% of TD. The density greatly affects the resistance of degradation together with a leakage current. This will be discussed later in more detail. As a whole, the ceramics sintered at 1300°C were found to comprise many pores, compared with the ceramics at 1350°C, as shown in SEM micrographs in Fig. 2. The average grain size was found to decrease in the range of 7.4 to 6.3 μm at 1300°C and 18.2 to 8.7 μm at 1350°C with increasing Dy_2O_3 content. It is believed that the decrease of the average grain size with Dy_2O_3 content is attributed to segregation of Dy_2O_3, which is nearly insoluble in ZnO grains, to grain boundaries. This was nearly equal to that of ceramics doped with other rare-earth metal oxides.

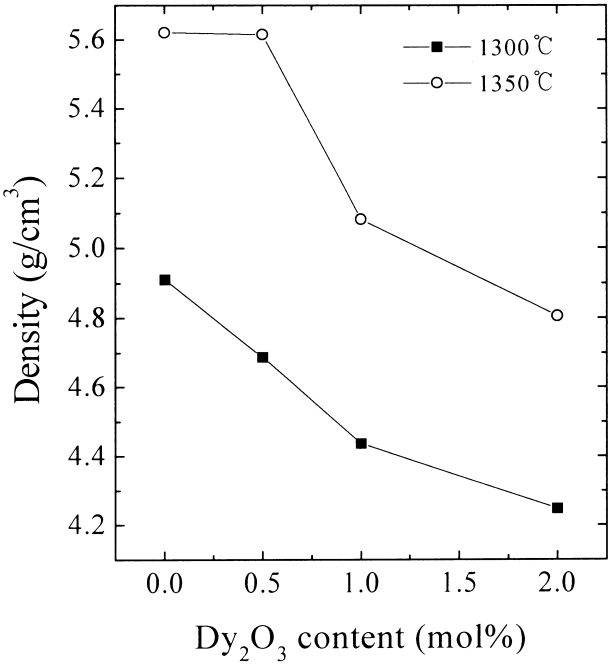

Fig. 1. The density of ZPCD ceramics with Dy_2O_3 content.

The electrical properties of the ZnO varistors were characterized by their electric field–current density (E–J) properties. Fig. 3 shows the E–J properties of ZPCD varistors. The dependence of Dy_2O_3 content on the E–J characteristics was far stronger at 1350°C than at 1300°C. In other words, the characteristic curves were collected in one place at 1300°C, whereas they were scattered at 1350°C. The variation of the more detailed V–I characteristic parameters, such as varistor voltage ($V_{1\ mA}$), varistor voltage per grain boundaries (V_{gb}), nonlinear exponent (α), and leakage current (I_ℓ) with Dy_2O_3 content is shown in Fig. 4. The value of $V_{1\ mA}$ was increased in the range of 337.4 to 560.9 V/mm at 1300°C and 8.85 to 404.3 V/mm at 1350°C with increasing Dy_2O_3 content. The V_{gb} is defined by $V_{gb} = (d/D)\ V_{1\ mA}$, where d is the average grain size and D is the thickness of sample. The value of V_{gb} was also increased in the range of 2.5 to 3.5 V/gb at 1300°C and 0.2 to 3.5 at 1350°C with increasing Dy_2O_3 content. The varistors with Dy_2O_3 content agreed to generally well-known 2–4 V/gb. The value of α, in varistors sintered at 1300°C without Dy_2O_3, was calculated to be 29.7, whereas it, in varistors with Dy_2O_3, was largely increased in the range of 39.2 to 53.9 with increasing Dy_2O_3 content. In particular, the varistors with 2.0 mol% Dy_2O_3 exhibited the best nonlinear V–I characteristics, in which the value of α and I_ℓ is 53.9 and 11.7 μA, respectively. On the other hand, the value of α, in varistors sintered at 1350°C without Dy_2O_3, was very poor, only 2, whereas, in varistors with Dy_2O_3 was in the range of 37.8 to 39.7 with increasing Dy_2O_3 content. In particular, the varistors with 0.5 mol% Dy_2O_3 exhibited the best nonlinear V–I characteristics, in which the value of α and I_ℓ is 37.8 and 5.4 μA, respectively. It can be seen that ZnO varistors are greatly improved at both sintering temperatures when Dy_2O_3 is incorporated into the ZnO–Pr_6O_{11}–CoO ternary system.

The existence of a Schottky barrier at grain boundary has been inferred from the voltage dependence of the capacitance. In other words, the higher the applied voltage, the lower the capacitance. The relation of $1/C_b^2$ versus V_{gb} is shown in Fig. 5. The variation of the more detailed C–V characteristic parameters, such as donor concentration (N_d), depletion layer width (t), density of interface states (N_t), and barrier height (ϕ_b) is shown in Fig. 6. The value of N_d was decreased in the range of 1.67×1018 to 0.31×10^{18} cm^{-3} at 1300°C and 14.61×10^{18} to 0.55×10^{18} cm^{-3} at 1350°C with increasing Dy_2O_3 content. This does not greatly differ from the general $\sim10^{18}$ magnitude order. This shows that Dy_2O_3 acts as an acceptor. Although Dy^{+3} ions have a larger radius (0.091 nm) than Zn^{+2} ions (0.074 nm), limited

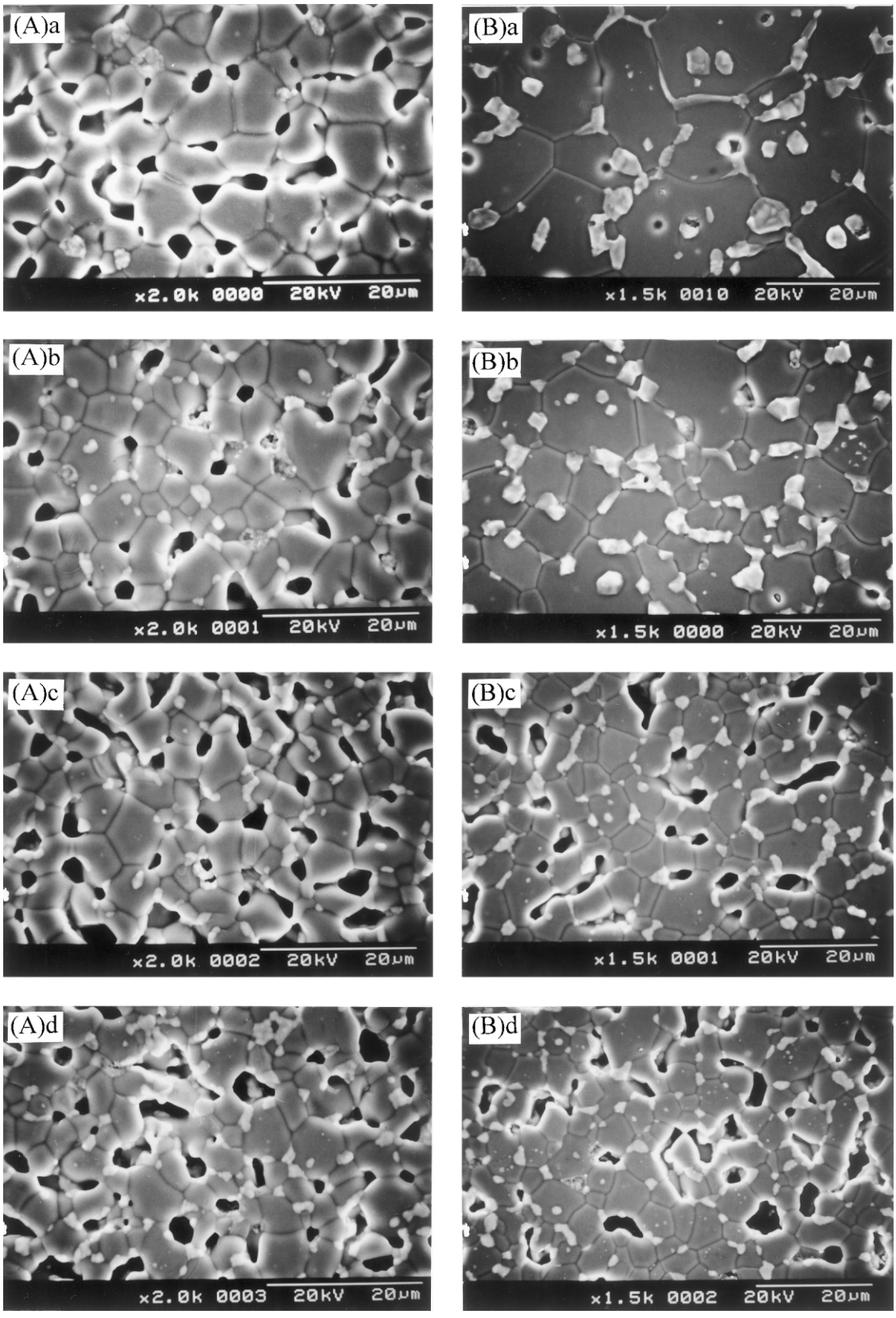

Fig. 2. SEM micrographs of ZPCD ceramics with Dy_2O_3 content sintered at (A) 1300°C and (B) 1350°C. a: 0.0 mol%, b: 0.5 mol%, c: 1.0 mol%, and d: 2.0 mol%.

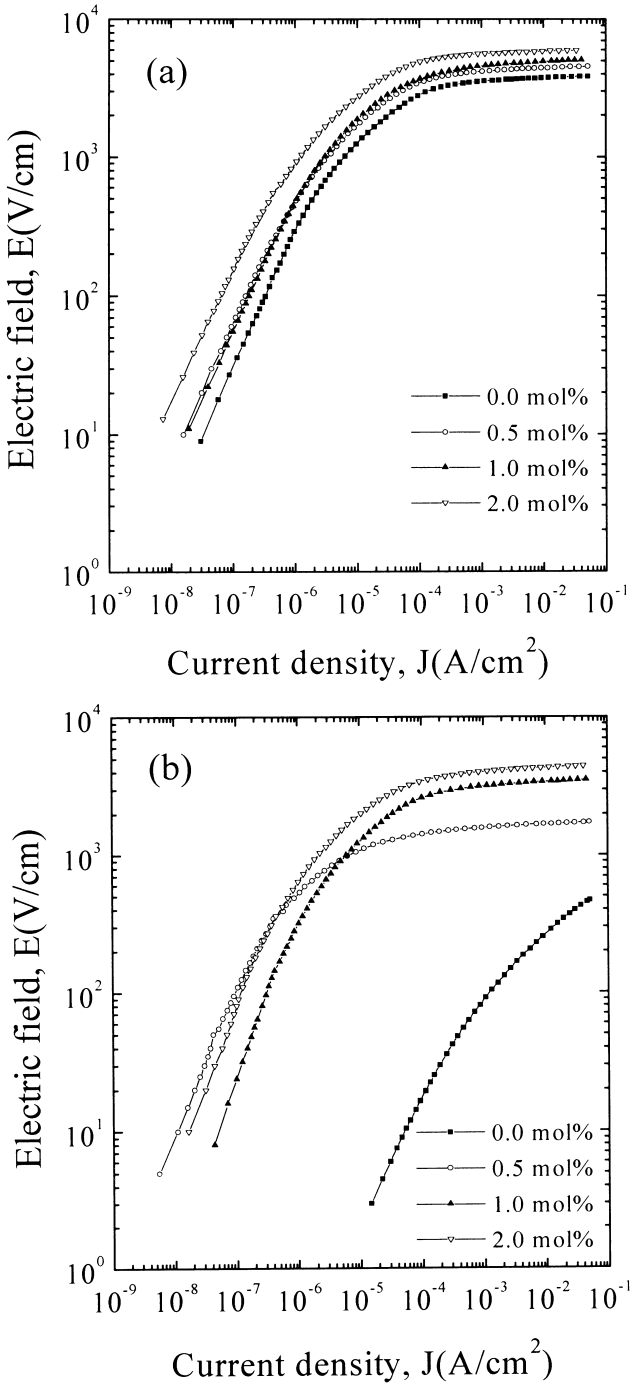

Fig. 3. The electric field–current density (E–J) characteristics of ZPCD varistors with Dy_2O_3 content sintered at (a) 1300°C and (b) 1350°C.

substitution within the ZnO grains is possible. Dy substitutes for Zn and creates lattice defect in ZnO grains. The chemical-defect reaction using the Kröger–Vink notation can be written as

$$Dy_2O_3 \xrightarrow{ZnO} 2Dy^{\bullet}_{Zn} + V''_{Zn} + 2O^{\times}_{O} + 1/2O_2,$$

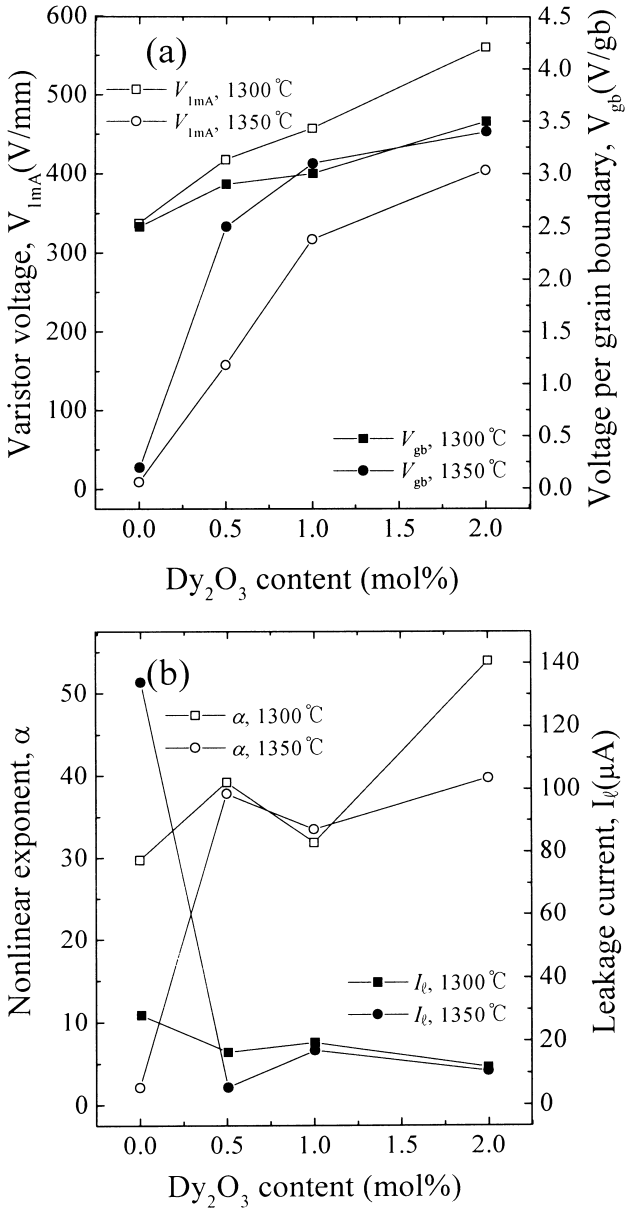

Fig. 4. The variation of (a) varistor voltage ($V_{1\ mA}$) and varistor voltage per grain boundaries (V_{gb}) and (b) nonlinear exponent (α) and leakage current (I_ℓ) of ZPCD varistors with Dy_2O_3 content.

where $Dy^{\bullet}_{Zn}$ is a positively charged Dy ion substituted for Zn lattice site, V''_{Zn} is a negatively doubly charged Zn vacancy, and $O^{\times}_{O}$ is a neutral oxygen of oxygen lattice site. The oxygen generated in the reaction above affects the donor concentration. In other words, N_d is related to the partial pressure of oxygen (P_{O_2}), namely, $N_d \propto P_{O_2}^{-1/4}$ or $P_{O_2}{}^{-1/6}$. It is, therefore, believed that the decrease of N_d with Dy_2O_3 content can be attributed to the increase in the partial pressure of oxygen. The increase of t for both sintering temperatures, with increasing Dy_2O_3 content, is attributed to the decrease of N_d. As Dy_2O_3 content increases, the value of N_t was decreased in the range of 3.64×10^{12} to 1.93×10^{12} cm^{-2}

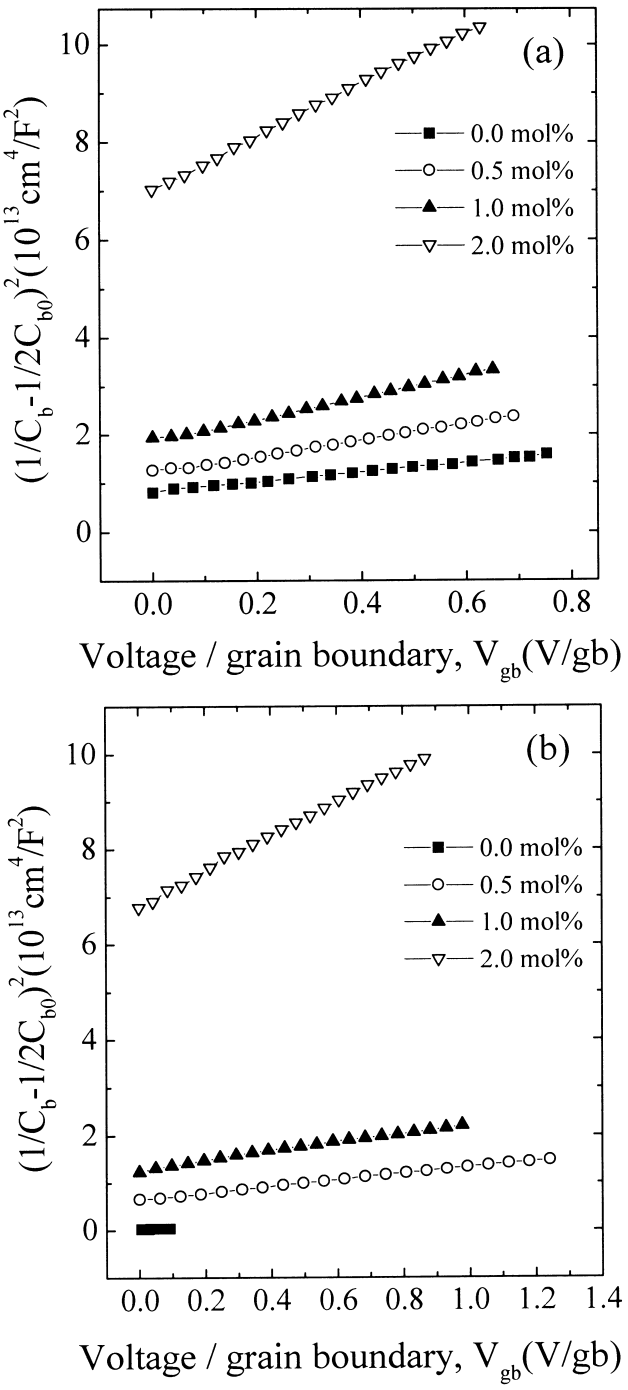

Fig. 5. The capacitance–voltage (C–V) characteristics of ZPCD varistors with Dy_2O_3 content sintered at (a) 1300°C and (b) 1350°C.

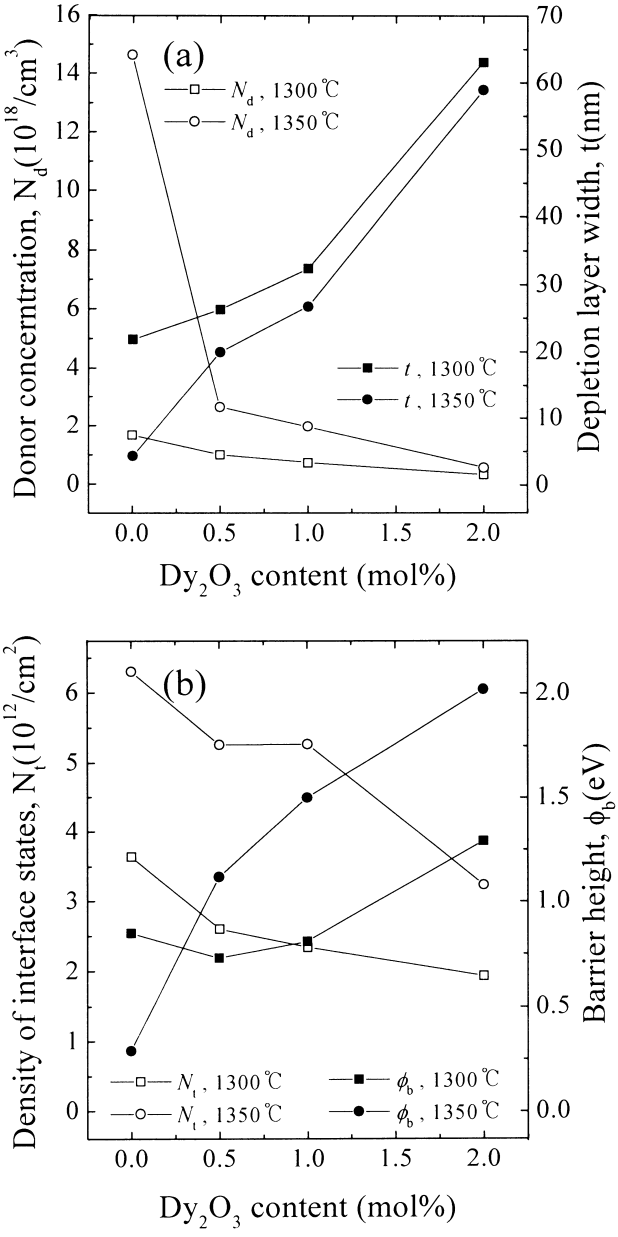

Fig. 6. The variation of (a) donor concentration (N_d) and depletion layer width (t) and (b) density of interface states (N_t) and barrier height (ϕ_b) of ZPCD varistors with Dy_2O_3 content.

at 1300°C and 6.30×10^{12} to 4.20×10^{12} cm^{-2} at 1350°C. The value of ϕ_b was increased in the range of 0.85 to 1.29 eV at 1300°C and 0.29 to 2.02 eV at 1350°C with increasing Dy_2O_3 content. The ϕ_b is directly connected with the N_d and N_t. In other words, the ϕ_b is estimated by the variation rate in the N_t and N_d. In general, the ϕ_b is increased with increasing N_t and decreasing N_d. If the variation rate of N_d is much larger than that of N_t with an additive content, the ϕ_b is much more strongly affected by the N_d than the N_t. This can explain why the ϕ_b is increased with increasing Dy_2O_3 content.

Fig. 7 shows the leakage current during the first d.c. stress of ZPCD varistors sintered at 1300°C. The varistors, even under relatively weak stress (first stress), exhibited the thermal runaway within short time. It is believed that this result is attributed to the low density of ceramics and the high leakage current. What is remarkable is that the degradation has appeared quickly in the order of low density. Therefore, it is clear that the density of ceramics affects the degradation more than the leakage current.

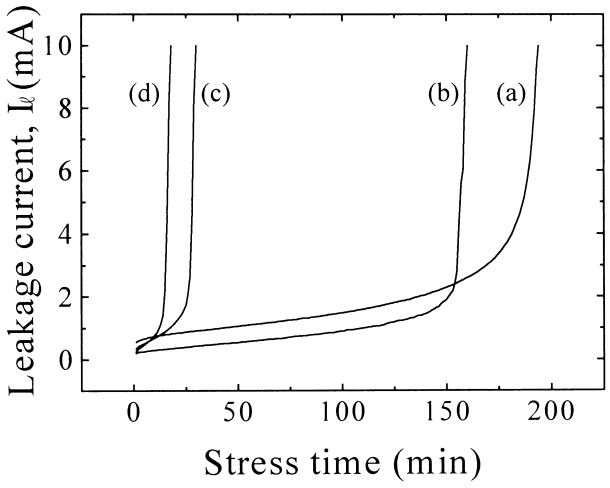

Fig. 7. The leakage current of ZPCD varistors with Dy_2O_3 content during the first d.c. stress sintered at 1300°C: (a) 0.0 mol%, (b) 0.5 mol%, (c) 1.0 mol%, and (d) 2.0 mol%.

Fig. 8 shows the leakage current during various stresses of ZPCD varistors sintered at 1350°C. First and foremost, it can be seen that ZPCD varistors, except for varistors with 2.0 mol% Dy_2O_3 sintered at 1350°C, are far more stable than any varistors sintered at 1300°C. It is believed that this can be attributed to the much higher density. Comparing varistors with 2.0 mol% Dy_2O_3 sintered at 1300°C with varistors with 1.0 mol% Dy_2O_3 sintered at 1350°C, it can be clearly seen that the density has a greater effect than the leakage current. The varistors without Dy_2O_3 exhibited weak positive creep phenomena of the leakage current with various stresses. Moreover, they showed rather negative creep phenomena during the fifth stress. Although they have a very high leakage current, to not appear the thermal runaway is likely to due to ohmic-like properties, which is extremely low nonlinearity. The varistors with 1.0 and 2.0 mol% Dy_2O_3 exhibited thermal runaway at the second and first stress, respectively. Meanwhile, the varistors with 0.5 mol% Dy_2O_3 did not exhibit the thermal runaway until the fourth stress. Therefore, the varistors with 0.5 mol% Dy_2O_3 are expected to show the best stability.

More detailed variations of *V–I* characteristic parameters after various stresses are summarized in Table 1. For the varistors without Dy_2O_3, the variation rate of the varistor voltage ($\%\Delta V_{1\ mA}$) was beyond −10%, even after the first stress. The varistors with 0.5 mol% Dy_2O_3 exhibited very good stability having $\%\Delta V_{1\ mA} = -1.7\%$ after the fourth stress. In the light of general facts that the allowed specifications of $\%\Delta V_{1\ mA}$ under d.c. stress in the commercial varistors are less than ±10%, it can be seen that the varistors with 0.5 mol% Dy_2O_3 possess excellent stability.

The degradation of ZnO varistors is associated with the lowering of the potential barrier at the grain boundaries, which is related to the annihilation of interface defect states, when stressed continuously by an electric field. So far, among mechanisms proposed to explain the degradation, the most probable mechanism is accepted to be the ion migration mechanism proposed by Gupta and Carlson.[14] According to this, when ZnO varistors are stressed continuously by an electric field, the positively charged zinc interstitial (Zn_i) formed and

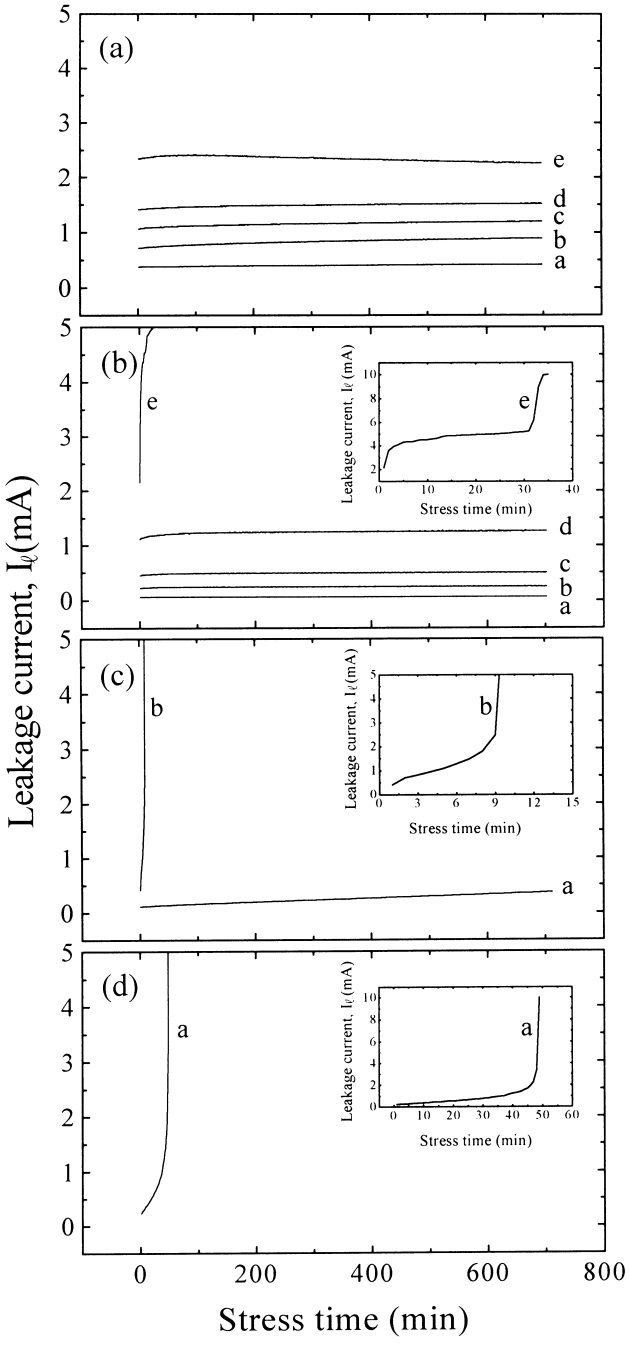

Fig. 8. The leakage current of ZPCD varistors with Dy_2O_3 content during various d.c. stresses sintered at 1350°C: (a) 0.0 mol%, (b) 0.5 mol%, (c) 1.0 mol%, and (d) 2.0 mol%. a: The first stress, b: the second stress, c: the third stress, d: the fourth stress, and e: the fifth stress.

Table 1
The variation of V–I characteristic parameters in ZPCD varistors with Dy_2O_3 content before and after various d.c. stresses sintered at 1350°C

Dy_2O_3 content (mol%)	Stress conditions	$V_{1\ mA}$ (V/mm)	$\%\Delta V_{1\ mA}$	α	$\%\Delta\alpha$	I_ℓ (μA)	$\%\Delta I_\ell$
0.0	Before	8.9	0	2.1	0	133.8	0
	First	7.9	−11.2	2.0	−4.8	135.6	1.3
	Second	6.5	−27.0	1.9	−9.5	139.1	4.0
	Third	5.8	−34.8	1.8	−14.3	140.2	4.8
	Fourth	5.4	−39.3	1.8	−14.3	141.1	5.5
	Fifth	5.4	−39.3	1.8	−14.3	140.6	5.1
0.5	Before	158.2	0	37.8	0	5.4	0
	First	157.9	−0.2	36.9	−2.4	6.2	14.8
	Second	157.2	−0.6	36.2	−4.2	6.9	27.8
	Third	156.6	−1.0	35.4	−6.3	7.5	38.9
	Fourth	155.5	−1.7	33.8	−10.6	8.3	53.7
	Fifth			Thermal runaway			
1.0	Before	317.3	0	33.4	0	17.0	0
	First	304.7	−4.0	24.2	−27.5	28.4	67.0
	Third			Thermal runaway			
2.0	Before	404.3	0	39.7	0	10.5	0
	First			Thermal runaway			

frozen in the depletion layer, during cooling from sintering temperature, migrates toward the negatively charged grain boundary interface, and it recombines with zinc vacancy (V_{Zn}) there. As a result, the recombination of these species leads to the degradation of ZnO varistors. In the light of these facts, it is possible that the reason why Dy_2O_3 doped Pr_6O_{11}-based ZnO varistors exhibit predominant degradation characteristics is because the added Dy_2O_3 spatially restricts the migration of zinc interstitial (Zn_i) within the depletion layer or stabilizes the interface states.

4. Conclusions

The electrical properties and degradation characteristics of Pr_6O_{11}-based ZnO varistors, which are composed of ZnO–Pr_6O_{11}–CoO-Dy_2O_3 systems, were investigated according to Dy_2O_3 content at sintering temperature 1300 and 1350°C. The ceramics sintered at 1350°C were far more densified than those at 1300°C and highly densified ceramics were obtained by doping with 0.5 mol% Dy_2O_3. The addition of Dy_2O_3 to the ternary system ZnO–Pr_6O_{11}–CoO greatly improved the V–I characteristics in terms of with and without Dy_2O_3 addition. All the varistors sintered at 1300°C were completely degraded even under relatively weak stress, which exhibited the thermal runaway within a short time in order of low density. On the contrary, the stability of varistors sintered at 1350°C was far higher than that at 1300°C. In particular, the varistors with 0.5 mol% Dy_2O_3 showed excellent stability, as well as relatively good nonlinear V–I characteristics. The variation rate of varistor voltage was −1.7%, even under very severe stress such as $(0.80\ V_{1\ mA}/90°C/12\ h)+(0.85\ V_{1\ mA}/115°C/12\ h)+(0.90\ V_{1\ mA}/120°C/12\ h)+(0.95\ V_{1\ mA}/125°C/12\ h)$.

Consequently, it was estimated that the 98.0 mol% ZnO-0.5 mol% Pr_6O_{11}-1.0 mol% CoO-0.5 mol% Dy_2O_3 based ceramic material will be usefully used in the future as a basic composition to develop the advanced Pr_6O_{11}-based ZnO varistors, having good performance and stability.

Acknowledgements

This work was performed by the Electrical Engineering and Science Research Institute (EESRI) under the support of Korea Electric Power Corporation (KEPCO) in 1999 (No. 99-016).

References

1. Levinson, L. M. and Pilipp, H. R., Zinc oxide varistor — a review. *Am. Ceram. Soc. Bull.*, 1986, **65**, 639–646.
2. Gupta, T. K., Application of zinc oxide varistor. *J. Am. Ceram. Soc.*, 1990, **73**, 1817–1840.
3. Lee, Y. S. and Tseng, T. Y., Phase identification and electrical properties in ZnO-glass varistors. *J. Am. Ceram. Soc.*, 1992, **75**, 1636–1640.
4. Mukae, K., Zinc oxide varistors with praseodymium oxide. *Am. Ceram. Soc. Bull.*, 1987, **66**, 1329–1331.
5. Alles, A. B. and Burdick, V. L., The effect of liquid-phase sintering on the properties of Pr_6O_{11}-based ZnO varistors. *J. Appl. Phys.*, 1991, **70**, 6883–6890.
6. Alles, A. B., Puskas, R., Callahan, G. and Burdick, V. L., Compositional effect on the liquid-phase sintering of praseodymium oxides-based ZnO varistors. *J. Am. Ceram. Soc.*, 1993, **76**, 2098–2102.
7. Lee, Y.-S., Liao, K.-S. and Tseng, T.-Y., Microstructure and crystal phases of praseodymium in zinc oxide varistor ceramics. *J. Am. Ceram. Soc.*, 1996, **79**, 2379–2384.

8. Nahm, C.-W. and Park, C.-H., Microstucture, electrical properties, and degradation behavior of praseodymium oxides-based zinc oxide varistors doped with Y_2O_3. *J. Mater. Sci.*, 2000, **35**, 3037–3042.
9. Nahm, C.-W., Park, C.-H. and Yoon, H.-S., Microstructure and varistor properties of ZnO–Pr_6O_{11}–CoO-Nd_2O_3 based ceramics. *J. Mater. Sci. Lett.*, 2000, **19**, 271–274.
10. Nahm, C.-W., Park, C.-H. and Yoon, H.-S., Highly stable non-ohmic characteristics of ZnO–Pr_6O_{11}–CoO-Dy_2O_3 based varistors. *J. Mater. Sci. Lett*. 2000, **19**, 725–728
11. Mukae, M., Tsuda, K. and Nagasawa, I., Capacitance-vs-voltage characteristics of ZnO varistor. *J. Appl. Phys*., 1979, **50**, 4475–4476.
12. Hozer, L., Semiconductor Ceramics: Grain Boundary Effects. Ellis Horwood, 1994, pp. 22.
13. Wurst, J. C. and Nelson, J. A., Lineal intercept tec-hnique for measuring grain size in two-phase polycrystalline ceramics. *J. Am. Ceram. Soc*., 1972, **97**(12), 109–111.
14. Gupta, T. K. and Carlson, W. G., A grain boundary defect model for instability/stability of a ZnO varistor. *J. Mater. Sci*., 1985, **20**, 3487–3500.